Accepted Manuscript

Inhibition of glycogen catabolism induces intrinsic apoptosis and augments multikinase inhibitors in hepatocellular carcinoma cells

Shrikant Barot, Ehab M. Abo-Ali, Daisy L. Zhou, Christian Palaguachi, Vikas V. Dukhande

PII: S0014-4827(19)30258-7

DOI: https://doi.org/10.1016/j.yexcr.2019.05.017

Reference: YEXCR 11436

To appear in: *Experimental Cell Research*

Received Date: 4 April 2019

Revised Date: 10 May 2019

Accepted Date: 14 May 2019

Please cite this article as: S. Barot, E.M. Abo-Ali, D.L. Zhou, C. Palaguachi, V.V. Dukhande, Inhibition of glycogen catabolism induces intrinsic apoptosis and augments multikinase inhibitors in hepatocellular carcinoma cells, *Experimental Cell Research* (2019), doi: https://doi.org/10.1016/j.yexcr.2019.05.017.

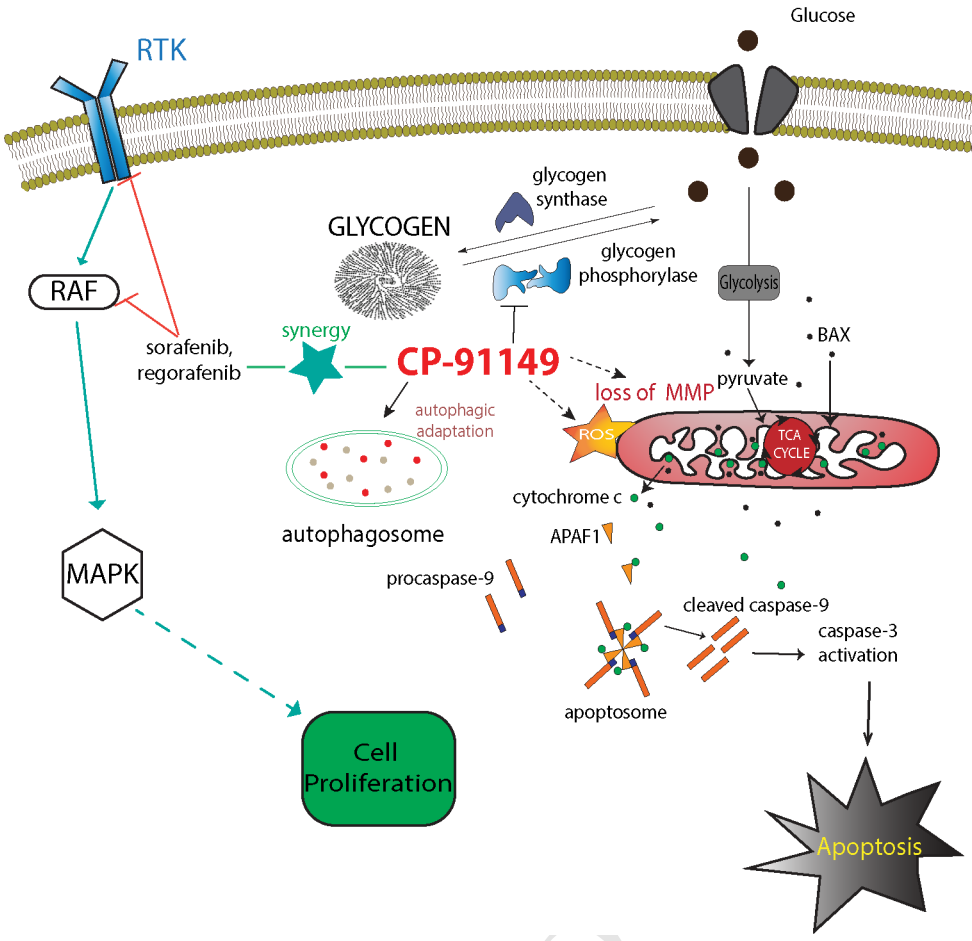
Glucose
RTK
glycogen synthase
GLYCOGEN
glycogen phosphorylase
Glycolysis
RAF
sorafenib, regorafenib
synergy
CP-91149
BAX
pyruvate
loss of MMP
autophagic adaptation
ROS
TCA CYCLE
cytochrome c
autophagosome
APAF1
MAPK
procaspase-9
cleaved caspase-9
caspase-3 activation
apoptosome
Cell Proliferation
Apoptosis

Inhibition of glycogen catabolism induces intrinsic apoptosis and augments multikinase inhibitors in hepatocellular carcinoma cells

Shrikant Barot[a], Ehab M. Abo-Ali[a], Daisy L. Zhou[b], Christian Palaguachi[b], and Vikas V. Dukhande[a, *]

[a] Department of Pharmaceutical Sciences, College of Pharmacy and Health Sciences, St. John's University, Queens, NY, USA

[b] Department of Biological Sciences, St. John's College of Liberal Arts and Sciences, St. John's University, Queens, NY, USA

[*] Corresponding Author: dukhandv@stjohns.edu

8000, Utopia Parkway,

SAH 141A, St. John's University,

Queens, NY, 11439

USA

Tel: 1-718-990-3389

ABSTRACT

Hepatocellular carcinoma (HCC) is one of the leading cancers in the world in incidence and mortality. Current pharmacotherapy of HCC is limited in the number and efficacy of anticancer agents. Metabolic reprogramming is a prominent feature of many cancers and has rekindled interest in targeting metabolic proteins for cancer therapy. Glycogen is a storage form of glucose, and the levels of glycogen have been found to correlate with biological processes in reprogrammed cancer cells. However, the contribution of glycogen metabolism to carcinogenesis, cancer cell growth, metastasis, and chemoresistance is poorly understood. Thus, we studied the processes involved in the inhibition of glycogen metabolism in HCC cells. Pharmacological inhibition of glycogen phosphorylase (GP), a rate-limiting enzyme in glycogen catabolism, by CP-91149 led to a decrease in HCC cell viability. GP inhibition induced cancer cell death through the intrinsic apoptotic pathway. Mitochondrial dysfunction and autophagic adaptations accompanied this apoptosis process whereas endoplasmic reticulum stress, necrosis, and necroptosis were not major components of the cell death. In addition, GP inhibition potentiated the effects of multikinase inhibitors sorafenib and regorafenib, which are key drugs in the advanced-stage HCC therapy. Our study provides mechanistic insights into cell death by perturbation of glycogen metabolism and identifies GP inhibition as a potential HCC pharmacotherapy target.

Keywords: Apoptosis; Autophagy; Glycogen phosphorylase; Hepatocellular carcinoma, Metabolic reprogramming; Sorafenib

1. Introduction

Liver cancer is the sixth most common cancer in the world and the third leading cause of cancer mortalities [1]. Hepatocellular carcinoma (HCC) is the most common form of liver cancer, accounting for more than 90% of these cases [2]. HCC treatment involves tumor resection and liver transplantation in the early stages of the disease whereas the multikinase, anti-angiogenic drugs sorafenib and regorafenib are employed with limited success in the advanced stages [1]. Thus, there is a dire need for novel therapeutics for HCC.

Metabolic reprogramming, a hallmark of many cancers, enables cancer cells to survive, proliferate, invade surrounding tissues, and metastasize to distant locations [3, 4]. Normal cells utilize glucose mainly by transitioning pyruvate generated by glycolysis to mitochondrial oxidative metabolism. On the contrary, cancer cells upregulate their glycolytic pathway even in the presence of sufficient molecular oxygen. This phenomenon, referred to as aerobic glycolysis, was first noted by Otto Warburg in the 1920s [5]. Warburg's observations went largely unnoticed for decades until recently, when an intimate connection between oncogenes and metabolism was discovered [6, 7]. The oncogenes *RAS* and *MYC* and the tumor suppressor *TP53* are known to rewire glucose metabolism [8]. Cancer cells have high biosynthetic demand due to their increased proliferation, shifting from the ATP generation-centric aerobic cellular respiration to pathways that provide the ability to synthesize nucleic- and fatty acids and confer protection from oxidative stress [9, 10]. In addition, metabolic reprogramming is known to promote tumor microenvironment acidification, making these metabolic pathway proteins valuable chemotherapy targets. In fact, a number of investigational drugs targeting glycolysis are currently being studied [11–15]. However, glycolysis is a central cellular energetic pathway, and significant toxicities associated with glycolytic inhibitors could restrain their development as suitable drugs. 3-bromopyruvate (3-BP) is a known inhibitor of glycolysis and has significant

anticancer properties. However, owing to 3-BP's total energy metabolism blockade, it was suspected to be the agent that resulted in the death of three patients at an alternative medicine facility in Germany [11, 16]. Alternatively, glycogen, a vital energy supply for cancer cells, may be a more suitable pharmacotherapy target.

Glycogen is a soluble polymer of glucose that has α-1,4 glucosidic linkages and branches occurring every 12-14 residues via an α-1,6 glucosidic linkage. Glycogen is synthesized by the actions of glycogen synthase and glycogen branching enzyme, and it is catabolized by glycogen phosphorylase (GP) and glycogen debranching enzyme (GDE). The liver is the second largest storage site for glycogen and plays an important role in maintaining blood glucose homeostasis [17]. The conversion of glycogen to glucose is used to maintain cellular glucose homeostasis. Hypoxia is one of the characteristics of solid tumors and is known to upregulate glycogen metabolism via glycogen synthase [18]. Glycogen is an essential metabolic cache in times of high cellular energy demand, such as hypoxia and increased metabolic activity. Indeed, glycogen is known to be upregulated in various cancers, and glycogen content inversely correlates with tumor proliferation [19]. Thus, glycogen can serve as a reserve for cancer cells during growth, proliferation, invasion, and metastasis as well as for survival during nutrient starvation [20, 21]. Increased glycogen stores are known to provide a survival advantage to neurons as well as cancers in hypoxic environments [22]. Depleting GP induces reactive oxygen species production, inhibits proliferation, and causes senescence in U87 and MCF-7 cells [23].

Several GP inhibitors are known, and CP-91149, an indole carboxamide allosteric inhibitor of GP, was developed as a potential antidiabetic drug. Indeed, CP-91149 treatment increased glycogen levels in human and rat hepatocytes [24, 25]. Few studies have investigated glycogen catabolism as a potential target for anticancer agents with emphasis on GP [23, 26] and GDE [27]. However, the precise role of GP in cancer biology and the mechanistic insights on

employing GP inhibitors for cancer therapy are not known. Patients with Hers disease, who have decreased liver GP activity, exhibit mild symptoms [28]. Therefore, GP inhibitors for HCC could result in less systemic toxicities than traditional chemotherapeutics. In the current study, we investigated the mechanism of CP-91149 treatment-induced cell death of HCC cells and determined whether CP-91149 could potentiate known and investigational anti-cancer agents.

2. Materials and methods

2.1. Reagents

Chemicals were purchased from the following sources: CP-91149, regorafenib, 2-deoxy-D-glucose, NS3694, and etoposide (ApexBio, Houston, USA); carbonyl cyanide 3-chlorophenylhydrazone (CCCP) (Tocris Bioscience, Minneapolis, USA); 3-bromopyruvate and chloroquine (Alfa Aesar, Tewksbury, USA); 6-aminonicotinamide (Acros-Organics, New Jersey, USA); sorafenib (Fisher Scientific, Hampton, USA). Mitochondria/cytosol fractionation kit was from Biovision (Milpitas, USA). PYGL plasmid was from Origene (RC210683, Rockville, USA). Accutase solution, Propidium iodide (PI), Hoechst 33342 (HO), MitoTracker Red CMXRos, FxCycle PI/RNase staining solution, CM-H_2DCFDA, and CyQuant Direct Cell Proliferation Assay kit were from ThermoFisher Scientific (Waltham, USA). FITC-Annexin V apoptosis detection kit was purchased from BD Biosciences (Franklin Lakes, USA). All antibodies were from Cell Signaling Technology (Danvers, USA) except for the LC3B and α-tubulin antibodies, which were from Proteintech Group (Rosemont, USA).

2.2. Cell culture and transfection

Human hepatocellular carcinoma (HepG2 and Hep3B) and rat hepatocellular carcinoma (H4IIE) cells were grown in Dulbecco's Modified Eagle's Medium (DMEM) normal glucose (5.5 mM)

and supplemented with 10% v/v FBS. All drug treatments were carried out 16 hr after subculturing cells to about 70% confluency. Cells were transfected, where indicated, with a plasmid for the glycogen phosphorylase liver isoform (*PYGL*) by electroporation using Neon transfection system as per the manufacturer's protocol. Cells were treated with inhibitors after 24 hr of transfection.

2.3. Cell viability determination

Cell viability was determined using MTT dye (3-(4,5-dimethylthiazol-2-yl)-2,5-diphenyltetrazolium bromide) and neutral red dye (3-amino-7-dimethylamino-2-methyl-phenazine hydrochloride). Cells were incubated with drugs at indicated concentrations and time points. For the MTT assay, at the end of the drug treatments, cells were treated with 0.05% (w/v) MTT dye for 3 hr at 37°C. The formazan crystals were dissolved in DMSO and absorbance was measured at 570 nm using the SpectraMax M5e plate reader (Molecular Devices, Sunnyvale, USA). The neutral red assay was performed as described by Repetto et al. with minor modifications [29]. Briefly, at the end of the drug treatments, cells were incubated with 40 µg/ml neutral red dye for 3 hr at 37 °C. Cells were then destained using a solution (50% ethanol, 49% deionized water, and 1% glacial acetic acid). Absorbance was measured at 540 nm using SpectraMax M5e plate reader.

2.4. Cell proliferation assay

Cell proliferation was determined using the CyQuant Direct Proliferation Assay kit as per the manufacturer's protocol. Briefly, at the end of drug treatments, medium was carefully aspirated from each well without disturbing the cells. 50 µl of 2X detection reagent was added to each well

containing 50 µl medium containing cells for 1 hr at 37 °C. Fluorescence was measured using the Spark 10M plate reader.

2.5. FITC-Annexin V/PI assay

For apoptosis detection, HepG2 cells were dual-stained using the FITC-Annexin V apoptosis detection kit. Briefly, at the end of the drug treatments, cells were washed with PBS and detached using Accutase solution (Corning, Carlsbad, USA). Collected cells were further washed twice with cold PBS, resuspended in cold 1X binding buffer, and dual stained with FITC-Annexin V and PI in the dark at 25 °C for 15 min. Flow cytometry was immediately performed on cells using the BD Accuri C6 flow cytometer (BD Biosciences) and analyzed using FlowJo v.10 software.

2.6. HO-PI staining

At the end of CP-91149 treatment, HepG2 cells were incubated with PI (25 µg/mL) for 10 min in the dark. Next, cells were washed with PBS and incubated with HO dye (11.25 µg/mL). Images were taken immediately using the EVOS FL Auto Imaging System (ThermoFisher Scientific, Waltham, USA) and quantified using ImageJ 1.8.0 software.

2.7. Subcellular fractionation

Mitochondrial and cytoplasmic fractions were isolated using the Mitochondria/Cytosol fractionation kit according to the manufacturer's protocol. HepG2 cells were collected at the end of the treatments and washed with ice-cold PBS, then centrifuged at 600g for 5 min at 4 °C, followed by resuspension of pellet in 1X cytosol extraction buffer mix. An ice-cold dounce tissue grinder was used for cellular homogenization. The homogenates were centrifuged at 700g for 10

min at 4 °C, and the supernatants were collected and centrifuged at 10,000g for 30 min at 4 °C. The supernatant was considered the cytosolic fraction while the pellet was resuspended using the mitochondrial extraction buffer mix and was considered the mitochondrial fraction.

2.8. Western blotting

HepG2 cells were lysed by scraping in modified RIPA buffer (50 mM Tris pH 8.0, 150 mM NaCl, 1% v/v NP40, 0.5% w/v deoxycholate, 0.1% w/v SDS, 10% v/v glycerol, 10 mM NaF, 0.4 mM EDTA) with protease inhibitors. The lysates were cleared by centrifugation at 10,000g for 10 min. Next, Laemmli sample buffer containing SDS and β-mercaptoethanol was added and samples were denatured by heat. Subsequently, samples were separated on polyacrylamide gels and transferred to PVDF membrane and processed for Western blotting with chemiluminescence detection. Images were obtained using ChemiDoc MP imaging system (Bio-Rad) or Azure C500 imaging system and analyzed using ImageJ 1.8.0 software.

2.9. Mitochondrial membrane potential (MMP) assay

MMP was assessed using MitoTracker Red CMXRos according to the manufacturer's protocol. Briefly, at the end of CP-91149 treatment, HepG2 cells were washed twice with PBS and incubated with MitoTracker Red CMXRos dye (100 nM) prepared in serum-free medium for 30 min at 37 °C. Cells were washed twice with PBS and fixed in 3.7% v/v formaldehyde in PBS for 15 mins. Cells were detached using Accutase solution and analyzed using the BD Accuri C6 flow cytometer and FCS Express 6 software.

2.10. Measurement of the total reactive oxygen species (ROS) levels

Cellular oxidative stress was evaluated using the chloromethyl derivative of 2′,7′-dichlorodihydrofluorescein diacetate (CM-H_2DCFDA). Briefly, at the end of the drug treatments, HepG2 cells were washed with PBS and detached using Accutase solution. Collected cells were washed twice with PBS, resuspended in serum-free medium, and stained with CM-H_2DCFDA (20 µM) for 30 min. at 37 °C in the dark. Flow cytometry was performed on cells using the Amnis FlowSight Imaging flow cytometer (MilliporeSigma, Burlington, USA) and analyzed using the Amnis IDEAS software to gate live and single positively-stained cells.

2.11. Cell cycle analysis

Cell cycle analysis was performed using the FxCycle PI/RNase Staining Solution. Briefly, at the end of the drug treatments, cells were washed twice with PBS and detached using Accutase solution. Cells were fixed using 70% ethanol at –20 °C overnight. Ethanol was removed from samples by centrifugation at 850 g and then cells were incubated with PI/RNase for 30 min. Subsequently, cells were analyzed using the BD Accuri C6 flow cytometer and FCS Express 6 software.

2.12. Immunofluorescence microscopy

HepG2 cells were cultured on poly-D-lysine-coated glass coverslips in 24-well cell culture plates. Cells were then treated with indicated drugs on the following day. Next, cells were washed with PBS and fixed using formaldehyde (3.7% v/v in PBS). Cells were permeabilized using cold Triton X-100 (0.25% v/v in PBS), for 5 minutes, washed, and incubated in FBS solution (10% v/v in PBS) for 1 hr. Next, samples were incubated with LC3B antibody overnight followed by washes and incubation with Alexa Fluor 594-conjugated secondary antibody. Coverslips were

mounted on slides using DAPI Fluoromount-G (SouthernBiotech), and images were taken using the EVOS FL Auto Imaging System (ThermoFisher Scientific).

2.13. Statistical analysis

Values are mean ± SEM of at least three independent experiments. Differences between groups are analyzed by one-way analysis of variances with either Dunnett's or Tukey post hoc test. The significance has been considered at *$p \leq 0.05$ and **$p \leq 0.01$. Data for Western blotting, imaging, and flow cytometry are representative of at least three independent determinations.

3. Results

3.1. CP-91149 decreases viability of hepatocellular carcinoma cells

We used an MTT cell viability assay in human (HepG2 and Hep3B)- and rat (H4IIE) hepatocellular carcinoma cells to examine the effects of the glycogen phosphorylase (GP) allosteric inhibitor CP-91149. Treatment with CP-91149 decreased the viability of HepG2, Hep3B, and H4IIE cells in a concentration-dependent manner, respectively (Fig. 1A-C). Etoposide, an anticancer agent, was used as a positive control in the experiment. In addition, we performed a neutral red dye uptake assay, which measures the capacity of viable cells to incorporate and bind to neutral red dye, in HepG2 and H4IIE cells. A concentration-dependent decrease in the viability of HepG2 and H4IIE cells by CP-91149 treatment was confirmed (Fig. 1D and Supplementary Fig. 1A, respectively). Next, we determined H4IIE cell viability via an MTT assay at various time points after CP-91149 treatment, which showed a time-dependent

decrease in cell viability (Fig. 1E). Based on these results, we chose the CP-91149 concentrations and treatment time to further investigate cell death mechanisms.

3.2. CP-91149 treatment decreases proliferation and alters the morphology of HepG2 cells

We measured the effect of CP-91149 treatment on HepG2 cell proliferation using CyQuant assay. HepG2 cells showed a significant reduction in cell proliferation after incubation with CP-91149 for 48 hr (Fig. 2A). CP-91149 toxicity was accompanied by altered morphology evident from the phase-contrast microscopy images of HepG2 (Fig. 2B) and H4IIE cells (Supplementary Fig. 1B). HepG2 cell size decreased in a concentration-dependent manner based on morphology, and this result was confirmed by the measurement of forward scatter in flow cytometry (Fig. 2C). Next, we transiently transfected a plasmid expressing the GP liver isoform (*PYGL*) by electroporation to check whether it could protect HepG2 cells from CP-91149 treatment. Our results showed a partial protection by *PYGL* from CP-91149 treatment (Fig. 2D), which could be explained by the limited transfection efficiency (49.1 ± 9.4 %) as evaluated by transfecting an EGFP-N3 plasmid, in HepG2 cells.

3.3. CP-91149 treatment induces apoptosis in HepG2 cells

Based on the morphological observations of HCC cells upon CP-91149 treatment, we hypothesized apoptosis as the primary cell death mechanism and therefore probed HCC cells with various markers of apoptosis. First, we performed annexin V-FITC / propidium iodide (PI) staining and flow cytometric analysis of HCC cells. The number of HepG2 cells in the early apoptotic phase (lower right quadrant) increased significantly upon CP-91149 treatment (Fig. 3A, B). In addition, we utilized HO-33342 (HO) and PI dye staining to delineate between apoptosis and necrosis processes via fluorescence microscopy. The HO dye enters live cells while PI can

enter only necrotic cells. In this assay, blue fluorescence indicates healthy cells, bright blue fluorescence denotes apoptotic cells, and necrotic cells exhibit red fluorescence. The number of apoptotic cells increased significantly upon CP-91149 treatment, whereas the higher CP-91149 concentrations of 75 μM and 100 μM showed mixed apoptotic-necrotic cells, a feature often present in late apoptotic cells (Fig. 3C, D).

3.4. Mitochondrial dysfunction leads to intrinsic apoptosis in CP-91149-treated HepG2 cells

We wanted to decipher the signaling pathway of apoptosis upon glycogen perturbations in HepG2 cells. Mitochondrial dysfunction and mitochondrial outer membrane permeabilization (MOMP), a process that leads to the leakage of mitochondrial intermembrane space proteins, often precedes the intrinsic pathway of apoptosis [30]. First, we measured the mitochondrial membrane potential (MMP) using MitoTracker Red CMXRos dye, the accumulation of which in the mitochondria is dependent upon MMP. We utilized carbonyl cyanide m-chlorophenyl hydrazine (CCCP), a protonophore uncoupler of oxidative phosphorylation, as a positive control that is known to dissipate MMP. Flow cytometric analysis revealed that MMP decreased significantly upon CP-91149 treatment in HepG2 cells (Fig. 4A). Next, we measured reactive oxygen species (ROS) levels as a marker to study oxidative stress. The number of HepG2 cells with higher levels of ROS increased upon CP-91149 treatment as evident by the rightward shift of the curve (Fig. 4B) and quantification of fluorescence intensity (Fig. 4C).

We performed subcellular fractionation of HepG2 cells and probed for the apoptotic markers in the mitochondrial and the cytosolic fractions using COX-IV and α-tubulin expression to assess the purity of the fractions, respectively. Upon CP-91149 treatment, the expression of Bax decreased in the cytosolic fraction and increased in the mitochondrial fraction (Fig. 4D, E), whereas the expression of cytochrome c increased in the cytosolic fraction and decreased in the mitochondrial fraction (Fig. 4D, E). The expression of cleaved caspase-3, an active form of the

executor caspase that leads to proteolysis of a large number of substrates, was determined in HepG2 cell lysate. A decrease in the expression of procaspase-3 and increase in the expression of cleaved caspase-3 upon CP-91149 treatment confirmed the occurrence of apoptosis (Fig. 4F, G). Next, we measured the expressions of caspase-8 and caspase-9 as markers of the extrinsic and the intrinsic apoptotic pathways, respectively. Procaspase-9 levels decreased, and cleaved caspase-9 levels increased; in addition, a modest increase in cleaved caspase-8 was observed upon CP-91149 treatment of HepG2 cells (Fig. 4F, G, and Supplementary Fig. 2A, B). Thus, our data identified that CP-91149 treatment induces the intrinsic pathway of apoptosis in HCC cells. NS3694 is an inhibitor of apoptosome formation and inhibits activation of procaspase-9 to caspase-9 [31]. To confirm the intrinsic apoptotic pathway as the mechanism of HepG2 cell death, we co-treated HepG2 cells with NS3694 and CP-91149 for 24 hr and performed MTT cell viability assay. NS3694 protected HepG2 cells from cell death induced by CP-91149 (Fig. 4H). Taken together, our data indicate that CP-91149 treatment results in ROS generation, mitochondrial dysfunction, and MOMP triggering the intrinsic pathway of apoptosis in HepG2 cells.

3.5. CP-91149 treatment induces autophagic adaptations in HepG2 cells

GP inhibition limits the availability of glucose from cellular glycogen. Therefore, we studied the effects of nutrient starvation and the involvement of autophagy in CP-91149-induced death of HepG2 cells. First, we performed an MTT cell viability assay in the presence of normal glucose (5.5 mM), high glucose (25 mM), and no glucose in CP-91149-treated cells. The cell viability assay was performed in the presence or absence of pyruvate (1 mM) in DMEM medium with glutamine to delineate the effects of CP-91149 on glucose energy metabolism. HepG2 cell viability was maximum in normal glucose medium, followed by high glucose medium, and the lowest in no glucose medium (Supplementary Fig. 3A). HepG2 viability was moderately lower in

medium without pyruvate. However, alterations in both glucose levels and pyruvate did not have a major impact on CP-91149 treatment in HepG2 cells (Supplementary Fig. 3A, B). Our findings on nutrient starvation experiments were surprising as we expected these treatments to bolster the effects of CP-91149 in HepG2 cells. Autophagic adaptations could explain the inability of nutrient starvation strategies to bolster CP-91149 effects. Thus, we hypothesized that autophagic adaptations in response to CP-91149 dampen the efficacy of the drug. Cytosolic LC3 is conjugated with phosphatidylethanolamine to form LC3-phosphatidylethanolamine conjugate (LC3-II) during autophagy. LC3II is then recruited to the autophagosome membrane, rendering it an appropriate marker of autophagy [32]. We studied endogenous LC3B localization by immunofluorescence microscopy in HepG2 cells. Tunicamycin induces endoplasmic reticulum stress associated autophagy and was used as a positive control. LC3B punctate localization increased with higher concentrations of CP-91149 (75 and 100 μM) indicating an increase in autophagy (Fig. 5A, B). To confirm the occurrence of autophagy, we measured the expression of LC3B and Beclin-1 by Western blotting, which showed an induction of autophagy upon CP-91149 treatment (Fig. 5C, D). Chloroquine, an agent that impairs lysosomal acidification and thereby blocks autophagy flux, was used as a positive control. Taken together, our results reveal that autophagy is an accompanying event in CP-91149-induced cell death in HepG2 cells.

3.6. Endoplasmic reticulum (ER) stress pathway, necrosis, and necroptosis are not key mediators of CP-91149-induced death in HepG2 cells

ER stress and the unfolded protein response are often implicated as accompanying factors in various pathophysiology and are known to result in cell death [33]. Therefore, we studied ER stress markers upon CP-91149 treatment in HepG2 cells. ER stress inducer tunicamycin was used as a positive control. Protein expression of JNK was unaltered and phospho-JNK levels at the expected sizes (54kDa and 46kDa) did not change upon CP-91149 treatment (Fig. 6A, B). Interestingly, we observed an additional band for phospho-JNK at 42kDa that showed high

expression only in CP-91149-treated cells (Fig. 6A). The significance of this band needs to be studied further. Expression of the chaperone Bip also did not change upon CP-91149 treatment (Fig. 6A, B). Therefore, we infer that ER stress is not the primary pathway for CP-91149 treatment-induced death of HepG2 cells.

Since HO-PI staining indicated the presence of necrosis at higher CP-91149 concentrations (Fig. 3C, D), we used a cytotoxicity assay based on the release of lactate dehydrogenase from cells to measure necrosis. The data showed the presence of necrosis only at 100 μM CP-91149 treatment (Fig. 6C). Next, we investigated whether the necrosis observed was secondary to apoptosis or necroptosis. We employed necrostatin-1, a RIP1 kinase inhibitor that blocks the programmed necroptosis process [34]. Co-treatment with necrostatin-1 did not protect HepG2 cells from the CP-91149-induced decrease in cell viability, indicating the absence of necroptosis (Fig. 6D). One of the key needs for the metabolic reprogramming of cancer cells is the constant supply of nucleotides for rapid proliferation. Thus, we determined whether inhibition of glycogen catabolism interferes with cell division in HepG2 cells. A PI-based flow cytometric determination of cell cycle analysis indicated that cells treated with lower concentrations of CP-91149 were arrested in the G_0/G_1 phase, and cells treated with 100 μM CP-91149 were arrested in the S phase (Fig. 6E, F). Therefore, our data indicate that CP-91149 induces concentration-dependent cell cycle alterations in HepG2 cells.

3.7. CP-91149 treatment is synergistic with multikinase, anti-angiogenic inhibitors that are vital for HCC treatment

The therapeutic potential of GP inhibitors for cancers depends on the premise that alterations of glycogen catabolism will affect cancer biology by augmenting the effect of current chemotherapeutics. Inhibition of distinct targets in metabolic pathways can result in

chemotherapy synergy as evident with the success of trimethoprim and sulfamethoxazole. Therefore, we tested whether GP inhibition can be synergistic with glycolysis or pentose phosphate pathway inhibition. Additionally, we tested CP-91149 for synergy with current indicated chemotherapeutics sorafenib and regorafenib for advanced-stage HCC. HepG2 cells were treated with CP-91149 in combinations with the multikinase inhibitors sorafenib and regorafenib, glycolysis inhibitors 2-deoxyglucose (2-DG) and 3-bromopyruvate (3-BP), and pentose phosphate pathway inhibitor 6-aminonicotinamide (6-AN). The combinations of CP-91149 with various inhibitors for their synergy profile was determined by the Chou-Talalay method combination index numbers, where a number lesser than 1 indicates synergy, 1 indicates no effect, and a number greater than 1 indicates antagonism [35]. CP-91149 combinations were synergistic with the multikinase inhibitors sorafenib and regorafenib (Fig. 7A-B, F-G). Notably, sorafenib and regorafenib are indicated for advanced-stage HCC, thus highlighting the potential of glycogen metabolic inhibition in HCC [2]. The combinations of CP-91149 with 2-DG, and 3-BP were not synergistic, indicating that they possibly target the same or similar signaling pathway(s) (Fig. 7C-D, H-I). The combination of CP-91149 with 6-AN was synergistic only at higher concentrations of CP-91149 employed (Fig. 7E, 7J).

4. Discussion

Cancer cells reprogram their glucose metabolism to fulfill increased cellular demand for proliferation, and the altered biological processes such as metastasis [3]. The reprogrammed glucose metabolism provides intermediates for nucleic acid biosynthesis, bolsters antioxidant defense, and augments amino acid biosynthesis [7]. Considerable efforts have been devoted to halt this reprogramming with metabolic inhibitors such as 3-bromopyruvate (3-BP), 2-deoxy-D-

glucose (2-DG), FX11, etc. [13]. Malignant tissues are known to store higher amounts of glycogen than their tissue of origin [36]. However, not much is known about the role of glycogen in cancer biology, limiting the ability to utilize glycogen metabolism as a chemotherapy target [37]. In this study, we demonstrated that treatment with CP-91149, an allosteric inhibitor of glycogen phosphorylase (GP), induced the intrinsic pathway of apoptosis-mediated cell death in HepG2 cells, along with a moderate involvement of autophagy (Fig. 8). Mitochondrial dysfunction and increased oxidative stress were observed in this cell death process whereas necrosis (other than the 'secondary necrosis' to apoptosis), necroptosis, and endoplasmic reticulum (ER) stress were not involved (Fig. 8). Interestingly, CP-91149 potentiated the effects of anticancer drugs such as multikinase, anti-angiogenic inhibitors sorafenib and regorafenib, and potential drugs like 6-aminonicotinamide, which targets the pentose phosphate pathway (Fig. 8). These combined findings suggest CP-91149 as a potential drug for the treatment for hepatocellular carcinoma (HCC).

Cancer treatment approaches such as chemotherapy, radiation, and immunotherapy all aim to induce death of cancer cells. Cell death by apoptosis is one of the important barriers to carcinogenesis as well as one of the key processes employed by chemotherapy drugs [38, 39]. Many cancer chemotherapy agents operate through the intrinsic/mitochondria-mediated pathway of apoptosis that is regulated by the BH3-domain family of pro- and anti-apoptotic proteins [39]. Activation of the intrinsic apoptosis pathway causes the release of cytochrome c from mitochondria, which binds to procaspase-9 and Apaf-1 and forms an apoptosome. Clustering of procaspase-9 in this fashion leads to the activation of caspase-9. Our study showed the presence of multiple markers of mitochondrial dysfunction and the intrinsic apoptosis in HepG2 cells induced by CP-91149 (Fig. 4). NS3694, an inhibitor of apoptosome formation, showed protection against cell death induced by CP-91149 (Fig. 4) [31]. Thus, we showed that the intrinsic pathway of apoptosis was the primary cell death mechanism induced by CP-91149

treatment in HepG2 cells. Some cancers are known to evade the apoptotic pathway and such resistance makes these cancers aggressive [40]. Because inhibition of glycogen metabolism induced apoptosis in HCC cells, this strategy could be studied in other apoptosis-resistant cancer cells [21].

The classical trigger for autophagy is nutrient starvation. Autophagy has been considered as a cell-protective mechanism, providing cells with essential nutrients in the conditions of deprivation [41]. Macroautophagy also recycles damaged cellular organelles such as mitochondria and thereby protects cells. However, recent research has shed light on the role of autophagy in the cell death process where autophagy either accompanies it or is considered as a causative factor [42]. The role of autophagy in cancer biology is not completely understood, with studies indicating both a protective pro-survival role and a growth-suppressing role as a causative factor in cell death [43]. Our study showed increased levels of LC3B-II expression and autophagosome formation at higher concentrations of CP-91149 (Fig. 5A, C). However, the cellular morphology did not resemble large-scale vacuole formation, and the increase in LC3 puncta was moderate. Hence, we conclude CP-91149-induced cell death accompanies autophagy but that the autophagic process itself is not a causative factor in this mechanism. The latter hypothesis is supported by a similar finding of overcoming autophagy in HCC cells for the glycolysis inhibitor 3-BP [44]. In addition, no significant augmentation of the effects of CP-91149 was observed when metabolic substrates such as glucose, and pyruvate were restricted (Supplementary Fig. S3). Moreover, the combinations of CP-91149 with the glycolytic inhibitors 2-DG and 3-BP were not synergistic (Fig. 6I). Thus, these findings indicate that there are marked differences in targeting glycolysis and glycogen metabolism. More studies are needed to delineate the differences between glycogen and glycolytic inhibitors in the context of cancer biology.

Most studies of CP-91149 have focused on its role in the management of diabetes where it was shown to be a specific inhibitor for GP causing glycogen accumulation [45]. However, only a handful of studies have investigated the inhibition of glycogen metabolism in cancer. In a key study, Favaro et al. showed that hypoxia in glioblastoma cell cultures or ischemia in tumor xenografts led to increased gene and protein expression of glycogen metabolic enzymes such as GP [23]. That study indicated that the silencing of GP in glioblastoma cells leads to oxidative stress and causes senescence through p53 activation [23]. Glycogen-metabolic proteins such as GP and glycogen synthase are key players in the hypoxic response of cancers and regulate cell survival and metastasis [23, 46, 47]. CP-320626, an indole carboxamide allosteric inhibitor of GP, induced defects in the pentose phosphate pathway, *de novo* fatty acid synthesis, and changes in cellular proteome in pancreatic cancer cells [48, 49]. Similarly, CP-91149 treatment increased glycogenosis and potentiated hormone therapy in prostate cancer [50]. Another study suggested the potential of blocking the glycogen debranching enzyme (GDE), involved in glycogen catabolism, for bladder cancer [51]. A recent study has also highlighted the key role of fibroblasts to alter tumor glycogen promoting proliferation and metastasis [52]. Collectively, these studies underline the importance of targeting glycogen metabolism for anticancer therapy.

Sorafenib (first-line) and regorafenib (second-line) are the only drugs indicated with survival benefits in advanced-stage hepatocellular carcinoma [1]. Sorafenib and regorafenib are multikinase inhibitors that block the signaling by RAF, VEGFR, and PDGFR thereby affecting proliferation signaling, angiogenesis, and apoptosis [53]. By inhibiting GP, CP-91149 acts on a different target than that of sorafenib and regorafenib. Our results showed synergy between CP-91149 and sorafenib or regorafenib, which could be due to targeting prominent cancer biological alterations such as proliferation signaling, angiogenesis, and metabolic reprogramming.

5. Conclusion

In the current study, we have shown that GP inhibition in HCC cells induces intrinsic apoptosis, mitochondrial dysfunction, and oxidative stress. Autophagic adaptations and cell cycle arrest accompanied those processes. The stimulus for the apoptosis could arise from the mitochondrial dysfunction and oxidative stress. Future studies could address the link between glycogen perturbations and mitochondrial dysfunction. Necrosis, necroptosis, and ER stress are largely absent in HCC cell death induced by CP-91149. To our knowledge, this is the first study to demonstrate the efficacy of metabolic inhibition in potentiating the multikinase, anti-angiogenic inhibitors sorafenib and regorafenib for HCC. Thus, our study elucidates the cell death mechanism of GP inhibition and highlights GP as a potential target for HCC.

Acknowledgements

This study was supported by faculty startup funds to VVD from the College of Pharmacy and Health Sciences, St. John's University. We thank Drs. Frank Barile and Xingguo Cheng for assistance with flow cytometry resources. We thank John Croft for carefully reviewing the manuscript.

Author Contributions

Conceived and designed the experiments: V.V.D., S.B., and E.M.A.; Performed the experiments: S.B., E.M.A., D.Z., and C.P.; Data analysis and figures: S.B., E.M.A., D.Z., and V.V.D.; Wrote the manuscript: V.V.D., E.M.A.

Declaration of interest

The authors declare no potential conflicts of interests.

Figure Legends

Fig. 1. CP-91149 treatment decreases the viability of hepatocellular carcinoma cells: Viability of A) HepG2, B) Hep3B, and C) H4IIE cells was determined by MTT assay after 24 hr incubation with increasing concentrations of CP-91149. Anticancer drug etoposide was used as a positive control. One-way ANOVA, n=3, **p<0.01. D) Viability of HepG2 cells was determined after 24 hr incubation with increasing concentrations of CP-91149 by neutral red dye uptake assay. Anticancer drug etoposide was used as a positive control. One-way ANOVA, n=3, **p<0.01 E) Viability of H4IIE cells was determined after incubation with CP-91149 or etoposide for the indicated time points using MTT assay. One-way ANOVA, n=3, *p<0.05, **p<0.01.

Fig. 2. CP-91149 treatment decreases the proliferation and alters morphology of HepG2 cells: A) Proliferation of HepG2 cells was determined using a CyQuant assay after 48 hr incubation with indicated concentrations of CP-91149. Anticancer drug etoposide was used as a positive control. One-way ANOVA, n=3, **p<0.01. B) Representative phase-contrast images from the morphological analysis of HepG2 cells after 24 hr incubation with etoposide or CP-91149. Scale bar: 200 μm. C) Effect of CP-91149 treatment on HepG2 cell size determined using flow cytometry. One-way ANOVA, n=3, **p<0.01. D) Viability of HepG2 cells was determined after transfection with either empty mammalian expression vector pcDNA 3.1 or a vector expressing liver isoform of glycogen phosphorylase *(PYGL)* and treatment on the next day with CP-91149 for 24 hr. One-way ANOVA, n=3, **p<0.01 compared with control, $^{\#\#}$p<0.01 compared between groups.

Fig. 3. CP-91149 treatment induces apoptosis in HepG2 cells: A) Annexin V-FITC and propidium iodide (PI) flow cytometry dot plots. HepG2 cells were treated with etoposide 80 µM or increasing concentration of CP-91149 for 24 hr and were then categorized based on the dye uptake as follows: viable cells (negative for annexin-V and PI), early apoptotic cells (positive for annexin-V only), late apoptotic cells (positive for both annexin-V and PI), and necrotic cells (positive for PI only). B) Quantitative data from flow cytometry experiment mentioned in (a). One-way ANOVA, n=4, *p<0.05, **p<0.01. C) Representative images of HepG2 cells stained with Hoechst-33342 (HO) and PI. HepG2 cells were treated with etoposide 80 µM or CP-91149 (25-100 µM) for 24 hr and then stained with HO and PI. Scale bar: 200 µm. D) Quantification of bright HO- and PI-positive cells was performed using FIJI plugin of ImageJ software. One-way ANOVA, n=3, $^{\#\#}$p<0.01, **p<0.01.

Fig. 3. Mitochondrial dysfunction and intrinsic apoptosis in CP-91149-treated HepG2 cells: A) Determination of mitochondrial membrane potential (MMP) of HepG2 cells using MitoTracker Red CMXRos dye. CCCP, an uncoupler of the oxidative phosphorylation, was used as a positive control. One-way ANOVA, n=3, **p<0.01. B) Flow cytometry histogram plots indicating the levels of reactive oxygen species via oxidation of CM-H_2DCFDA in HepG2 cells incubated with increasing concentration of CP-91149 for 24 hr. C) Quantitative data obtained from experiment outlined in B indicate mean DCF fluorescence intensity. One-way ANOVA, n=3, *p<0.05. D) Western blotting of indicated proteins from the mitochondrial and cytosolic fractions obtained from HepG2 cell lysates. COX-4 and tubulin show relative purity of fractions. E) Digitization of Western blot analysis performed in D using ImageJ software. One-way ANOVA, n=3, *p<0.05, **p<0.01. F) Representative images from the Western blotting of whole cell lysates obtained from HepG2 cells probed with cleaved caspase-3, cleaved caspase 8, and cleaved caspase-9 antibodies. G) Digitization of Western blot performed in F using ImageJ software. One-way

ANOVA, n=3, *p<0.05, **p<0.01. H) HepG2 cell viability using MTT assay after 24 hr treatment with indicated concentrations of CP-91149 and NS3694. One-way ANOVA, n=3, **p<0.01 compared with control, $^{\#\#}$p<0.01 compared between groups.

Fig. 5. CP-91149 treatment induces autophagic adaptations in HCC cells: A) Immunofluorescence staining of endogenous LC3B in HepG2 cells incubated with increasing concentration of CP-91149 or tunicamycin (10 µg/mL) for 24 hr. Tunicamycin induces endoplasmic reticulum stress-associated autophagy and was used as a positive control. Scale bar: 100 µm. Images are representative of three independent experiments. B) Quantification of LC3B-positive punctate fluorescence using imageJ software. One-way ANOVA, n=3, **p<0.01. C) HepG2 whole cell lysates after treatment with the indicated concentrations of CP-91149 for 24 hr were analyzed by Western blotting with LC3B and Beclin-1 antibodies. Autophagy flux inhibitor chloroquine was used as a positive control. D) Digitization of Western blot analysis performed in C using ImageJ software. One-way ANOVA, n=3, *p<0.05, **p<0.01.

Fig. 6. Endoplasmic reticulum (ER) stress pathway, necrosis, and necroptosis are not key mediators of CP-91149-induced death in HepG2 cells: A) Western blotting was employed to analyze the protein expression of ER stress markers phospho-JNK, JNK, and BiP from HepG2 cells treated with increasing concentration of CP-91149 or tunicamycin for 24 hr. ER stress inducer tunicamycin was used as a positive control. Images are representative from three independent experiments. B) Digitization of Western blotting performed in A using ImageJ software. One-way ANOVA, n=3, **p<0.01. C) Determination of lactate dehydrogenase release after 24 hr incubation with etoposide or increasing concentration of CP-91149. One-way ANOVA, n=3, **p<0.01. D) MTT Cell viability assay of HepG2 cells treated with CP-91149 and necrostatin-1 for 24 hr either alone or in combination is shown. One-way ANOVA, n=3,

**p<0.01. E) Representative flow cytometric data of cell cycle analysis from CP-91149 treated HepG2 cells. F) Representative quantification of cell cycle analysis data indicating percentage of cells in given phases. The experiment was replicated to confirm data.

Fig. 7. CP-91149 treatment potentiates the actions of the multikinase, anti-angiogenic inhibitors in HepG2 cells: Viability of HepG2 cells was determined after 24 hr incubation with CP-91149 alone or in combination with A) sorafenib, B) regorafenib, C) 2-deoxy-D-glucose (48 hr incubation), D) 3-bromopyruvate , and E) 6-aminonicotinamide. One-way ANOVA, n=3, *p<0.05, **p<0.01. F-J) Combination index values of indicated drugs was calculated by the Chou-Talalay method using CompuSyn software. A number lesser than 1 indicates synergy (green), 1 indicates no effect (yellow), and a number greater than 1 indicates antagonism (red).

Fig. 8. A schematic depicting cell death mechanism of CP-91149 in hepatocellular carcinoma cells: Allosteric inhibition of glycogen phosphorylase resulted in decreased viability of HepG2. Mitochondrial dysfunction was denoted by increased ROS generation, loss of mitochondrial membrane potential, and mitochondrial outer membrane permeabilization leading the release of cytochrome c. Subsequent activation of intrinsic apoptotic pathway led to cell death. Autophagic adaptations accompanied this process whereas primary necrosis, necroptosis, and ER stress were not involved. Glycogen metabolic inhibition synergized with multikinase inhibitors sorafenib and regorafenib and merits further investigation.

References

1. Forner A, Reig M, Bruix J (2018) Hepatocellular carcinoma. Lancet 391:1301–1314. https://doi.org/10.1016/S0140-6736(18)30010-2

2. Deng G-L, Zeng S, Shen H (2015) Chemotherapy and target therapy for hepatocellular carcinoma: New advances and challenges. World J Hepatol 7:787–798. https://doi.org/10.4254/wjh.v7.i5.787

3. Hanahan D, Weinberg RA (2011) Hallmarks of cancer: the next generation. Cell 144:646–74. https://doi.org/10.1016/j.cell.2011.02.013

4. Cairns RA, Harris IS, Mak TW (2011) Regulation of cancer cell metabolism. Nat Rev Cancer 11:85–95. https://doi.org/10.1038/nrc2981

5. Koppenol WH, Bounds PL, Dang CV (2011) Otto Warburg's contributions to current concepts of cancer metabolism. Nat Rev Cancer 11:325–37. https://doi.org/10.1038/nrc3038

6. Hsu PP, Sabatini DM (2008) Cancer cell metabolism: Warburg and beyond. Cell 134:703–7. https://doi.org/10.1016/j.cell.2008.08.021

7. Ward PS, Thompson CB (2012) Metabolic reprogramming: a cancer hallmark even warburg did not anticipate. Cancer Cell 21:297–308. https://doi.org/10.1016/j.ccr.2012.02.014

8. Ferreira LMR, Hebrant A, Dumont JE (2012) Metabolic reprogramming of the tumor. Oncogene 31:3999–4011. https://doi.org/10.1038/onc.2011.576

9. Vander Heiden MG, Cantley LC, Thompson CB (2009) Understanding the Warburg effect: the metabolic requirements of cell proliferation. Science 324:1029–1033. https://doi.org/10.1126/science.1160809

10. Schulze A, Harris AL (2012) How cancer metabolism is tuned for proliferation and vulnerable to disruption. Nature 491:364–73. https://doi.org/10.1038/nature11706

11. Ko YH, Verhoeven HA, Lee MJ, et al (2012) A translational study "case report" on the small molecule "energy blocker" 3-bromopyruvate (3BP) as a potent anticancer agent: from bench side to bedside. J Bioenerg Biomembr 44:163–70. https://doi.org/10.1007/s10863-012-9417-4

12. Chesney J, Clark J, Lanceta L, et al (2015) Targeting the sugar metabolism of tumors with a first-in-class 6-phosphofructo-2-kinase (PFKFB4) inhibitor. Oncotarget 6:18001–18011. https://doi.org/10.18632/oncotarget.4534

13. Gill KS, Fernandes P, O'Donovan TR, et al (2016) Glycolysis inhibition as a cancer treatment and its role in an anti-tumour immune response. Biochimica et Biophysica Acta (BBA) - Reviews on Cancer 1866:87–105. https://doi.org/10.1016/j.bbcan.2016.06.005

14. Pelicano H, Martin DS, Xu R-H, Huang P (2006) Glycolysis inhibition for anticancer treatment. Oncogene 25:4633–4646. https://doi.org/10.1038/sj.onc.1209597

15. Bhardwaj V, Rizvi N, Lai MB, et al (2010) Glycolytic Enzyme Inhibitors Affect Pancreatic Cancer Survival by Modulating Its Signaling and Energetics. Anticancer Res 30:743–749

16. Feldwisch-Drentrup H (2016) Candidate cancer drug suspected after death of three patients at an alternative medicine clinic. Science Insider

17. Bollen M, Keppens S, Stalmans W (1998) Specific features of glycogen metabolism in the liver. Biochem J 336:19–31

18. Pescador N, Villar D, Cifuentes D, et al (2010) Hypoxia promotes glycogen accumulation through hypoxia inducible factor (HIF)-mediated induction of glycogen synthase 1. PLoS One 5:e9644. https://doi.org/10.1371/journal.pone.0009644

19. Rousset M, Paris H, Chevalier G, et al (1984) Growth-related enzymatic control of glycogen metabolism in cultured human tumor cells. Cancer Res 44:154–60

20. Pelletier J, Bellot G, Gounon P, et al (2012) Glycogen Synthesis is Induced in Hypoxia by the Hypoxia-Inducible Factor and Promotes Cancer Cell Survival. Front Oncol 2:18. https://doi.org/10.3389/fonc.2012.00018

21. Curtis M, Kenny HA, Ashcroft B, et al (2019) Fibroblasts Mobilize Tumor Cell Glycogen to Promote Proliferation and Metastasis. Cell Metabolism 29:141-155.e9. https://doi.org/10.1016/j.cmet.2018.08.007

22. Saez I, Duran J, Sinadinos C, et al (2014) Neurons have an active glycogen metabolism that contributes to tolerance to hypoxia. J Cereb Blood Flow Metab. https://doi.org/jcbfm201433 [pii] 10.1038/jcbfm.2014.33

23. Favaro E, Bensaad K, Chong MG, et al (2012) Glucose utilization via glycogen phosphorylase sustains proliferation and prevents premature senescence in cancer cells. Cell Metab 16:751–64. https://doi.org/10.1016/j.cmet.2012.10.017

24. Somsak L, Czifrak K, Toth M, et al (2008) New inhibitors of glycogen phosphorylase as potential antidiabetic agents. Curr Med Chem 15:2933–83

25. Martin WH, Hoover DJ, Armento SJ, et al (1998) Discovery of a human liver glycogen phosphorylase inhibitor that lowers blood glucose in vivo. Proc Natl Acad Sci U S A 95:1776–81

26. Lee W-NP, Guo P, Lim S, et al (2004) Metabolic sensitivity of pancreatic tumour cell apoptosis to glycogen phosphorylase inhibitor treatment. Br J Cancer 91:2094–2100. https://doi.org/10.1038/sj.bjc.6602243

27. Guin S, Ru Y, Agarwal N, et al (2016) Loss of Glycogen Debranching Enzyme AGL Drives Bladder Tumor Growth via Induction of Hyaluronic Acid Synthesis. Clinical Cancer Research 22:1274–1283. https://doi.org/10.1158/1078-0432.CCR-15-1706

28. Hers HG and FVH (1968) Glycogen storage diseases: type II and type VI glycogenosis. In: Dickens F Randle, PJ and WJ Whelan (ed) Carbohydrate Metabolism and Its Disorders. Academic Press, New York

29. Repetto G, del Peso A, Zurita JL (2008) Neutral red uptake assay for the estimation of cell viability/cytotoxicity. Nat Protoc 3:1125–1131. https://doi.org/10.1038/nprot.2008.75

30. Green DR, Kroemer G (2004) The pathophysiology of mitochondrial cell death. Science 305:626–629. https://doi.org/10.1126/science.1099320

31. Lademann U, Cain K, Gyrd-Hansen M, et al (2003) Diarylurea Compounds Inhibit Caspase Activation by Preventing the Formation of the Active 700-Kilodalton Apoptosome Complex. Molecular and Cellular Biology 23:7829–7837. https://doi.org/10.1128/MCB.23.21.7829-7837.2003

32. Tanida I, Ueno T, Kominami E (2008) LC3 and Autophagy. In: Deretic V (ed) Autophagosome and Phagosome. Humana Press, Totowa, NJ, pp 77–88

33. Sano R, Reed JC (2013) ER stress-induced cell death mechanisms. Biochimica et Biophysica Acta (BBA) - Molecular Cell Research 1833:3460–3470. https://doi.org/10.1016/j.bbamcr.2013.06.028

34. Degterev A, Hitomi J, Germscheid M, et al (2008) Identification of RIP1 kinase as a specific cellular target of necrostatins. Nature Chemical Biology 4:313–321. https://doi.org/10.1038/nchembio.83

35. Chou T-C (2010) Drug combination studies and their synergy quantification using the Chou-Talalay method. Cancer Res 70:440–446. https://doi.org/10.1158/0008-5472.CAN-09-1947

36. Rousset M, Zweibaum A, Fogh J (1981) Presence of glycogen and growth-related variations in 58 cultured human tumor cell lines of various tissue origins. Cancer Res 41:1165–1170

37. Zois CE, Harris AL (2016) Glycogen metabolism has a key role in the cancer microenvironment and provides new targets for cancer therapy. J Mol Med (Berl) 94:137–54. https://doi.org/10.1007/s00109-015-1377-9

38. Fulda S, Debatin KM (2006) Extrinsic versus intrinsic apoptosis pathways in anticancer chemotherapy. Oncogene 25:4798–811. https://doi.org/10.1038/sj.onc.1209608

39. Adams JM, Cory S (2007) The Bcl-2 apoptotic switch in cancer development and therapy. Oncogene 26:1324–37. https://doi.org/10.1038/sj.onc.1210220

40. Igney FH, Krammer PH (2002) Death and anti-death: tumour resistance to apoptosis. Nature Reviews Cancer 2:277–288. https://doi.org/10.1038/nrc776

41. He C, Klionsky DJ (2009) Regulation mechanisms and signaling pathways of autophagy. Annu Rev Genet 43:67–93. https://doi.org/10.1146/annurev-genet-102808-114910

42. White E, DiPaola RS (2009) The double-edged sword of autophagy modulation in cancer. Clin Cancer Res 15:5308–16. https://doi.org/10.1158/1078-0432.CCR-07-5023

43. Sui X, Chen R, Wang Z, et al (2013) Autophagy and chemotherapy resistance: a promising therapeutic target for cancer treatment. Cell Death & Disease 4:e838. https://doi.org/10.1038/cddis.2013.350

44. Ganapathy-Kanniappan S, H Geschwind J-F, Kunjithapatham R, et al (2010) 3-Bromopyruvate Induces Endoplasmic Reticulum Stress, Overcomes Autophagy and Causes Apoptosis in Human HCC Cell Lines. Anticancer research 30:923–35

45. Treadway JL, Mendys P, Hoover DJ (2001) Glycogen phosphorylase inhibitors for treatment of type 2 diabetes mellitus. Expert Opin Investig Drugs 10:439–454. https://doi.org/10.1517/13543784.10.3.439

46. Winter SC, Buffa FM, Silva P, et al (2007) Relation of a Hypoxia Metagene Derived from Head and Neck Cancer to Prognosis of Multiple Cancers. Cancer Res 67:3441–3449. https://doi.org/10.1158/0008-5472.CAN-06-3322

47. Brahimi-Horn MC, Bellot G, Pouysségur J (2011) Hypoxia and energetic tumour metabolism. Current Opinion in Genetics & Development 21:67–72. https://doi.org/10.1016/j.gde.2010.10.006

48. Lee W-NP, Guo P, Lim S, et al (2004) Metabolic sensitivity of pancreatic tumour cell apoptosis to glycogen phosphorylase inhibitor treatment. Br J Cancer 91:2094–2100. https://doi.org/10.1038/sj.bjc.6602243

49. Ma D, Wang J, Zhao Y, et al (2012) Inhibition of Glycogen Phosphorylation Induces Changes in Cellular Proteome and Signaling Pathways in MIA Pancreatic Cancer Cells: Pancreas 41:397–408. https://doi.org/10.1097/MPA.0b013e318236f022

50. Schnier JB, Nishi K, Monks A, et al (2003) Inhibition of glycogen phosphorylase (GP) by CP-91,149 induces growth inhibition correlating with brain GP expression. Biochemical and Biophysical Research Communications 309:126–134. https://doi.org/10.1016/S0006-291X(03)01542-0

51. Ritterson Lew C, Guin S, Theodorescu D (2015) Targeting glycogen metabolism in bladder cancer. Nat Rev Urol 12:383–91. https://doi.org/10.1038/nrurol.2015.111

52. Curtis M, Kenny HA, Ashcroft B, et al (2019) Fibroblasts Mobilize Tumor Cell Glycogen to Promote Proliferation and Metastasis. Cell Metab 29:141-155.e9. https://doi.org/10.1016/j.cmet.2018.08.007

53. Bajetta E, Procopio G, Colombo A, et al (2009) Sorafenib in Hepatocellular Carcinoma. Clinical Medicine Therapeutics 1:CMT.S2314. https://doi.org/10.4137/CMT.S2314

Fig. 3

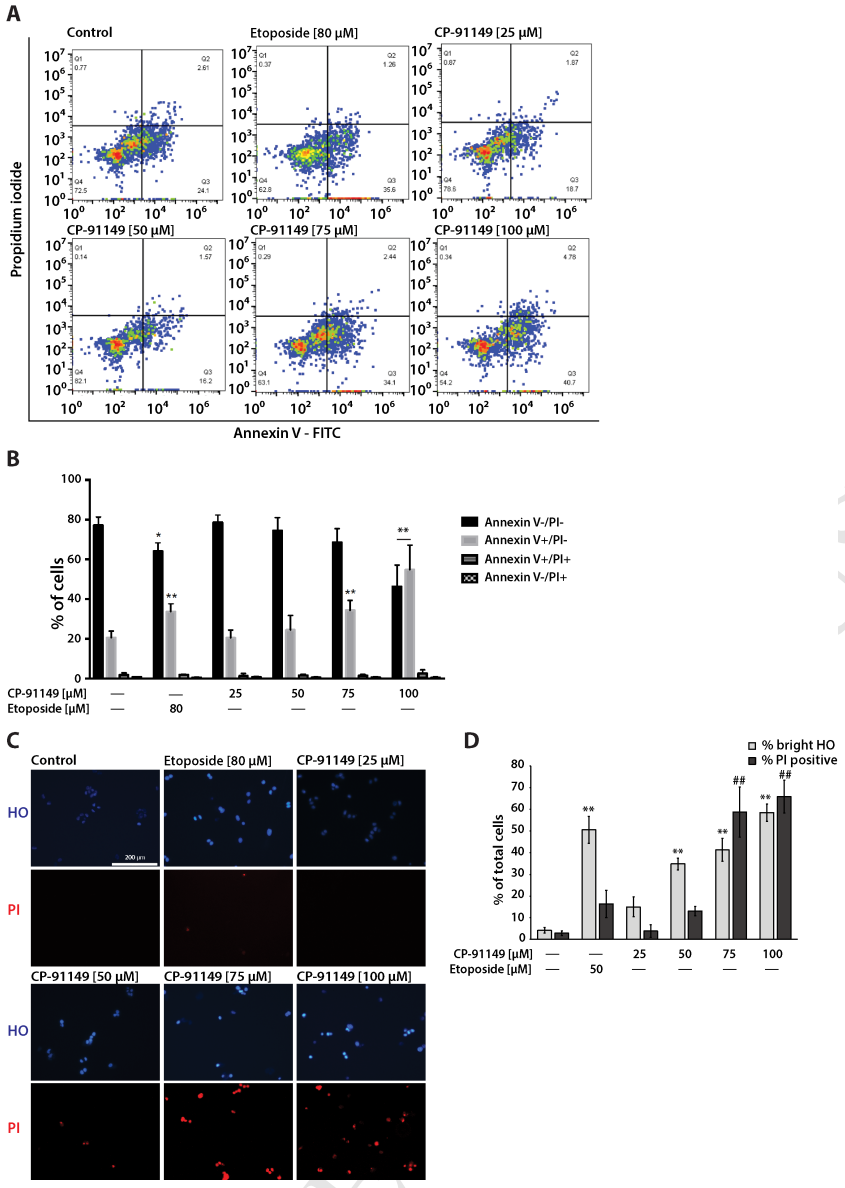
A
Control
Etoposide [80 µM]
CP-91149 [25 µM]
CP-91149 [50 µM]
CP-91149 [75 µM]
CP-91149 [100 µM]
Propidium iodide
Annexin V - FITC
B
% of cells
Annexin V-/PI-
Annexin V+/PI-
Annexin V+/PI+
Annexin V-/PI+
CP-91149 [µM]
Etoposide [µM]
C
Control
Etoposide [80 µM]
CP-91149 [25 µM]
CP-91149 [50 µM]
CP-91149 [75 µM]
CP-91149 [100 µM]
HO
PI
D
% bright HO
% PI positive
% of total cells
CP-91149 [µM]
Etoposide [µM]

Fig. 1

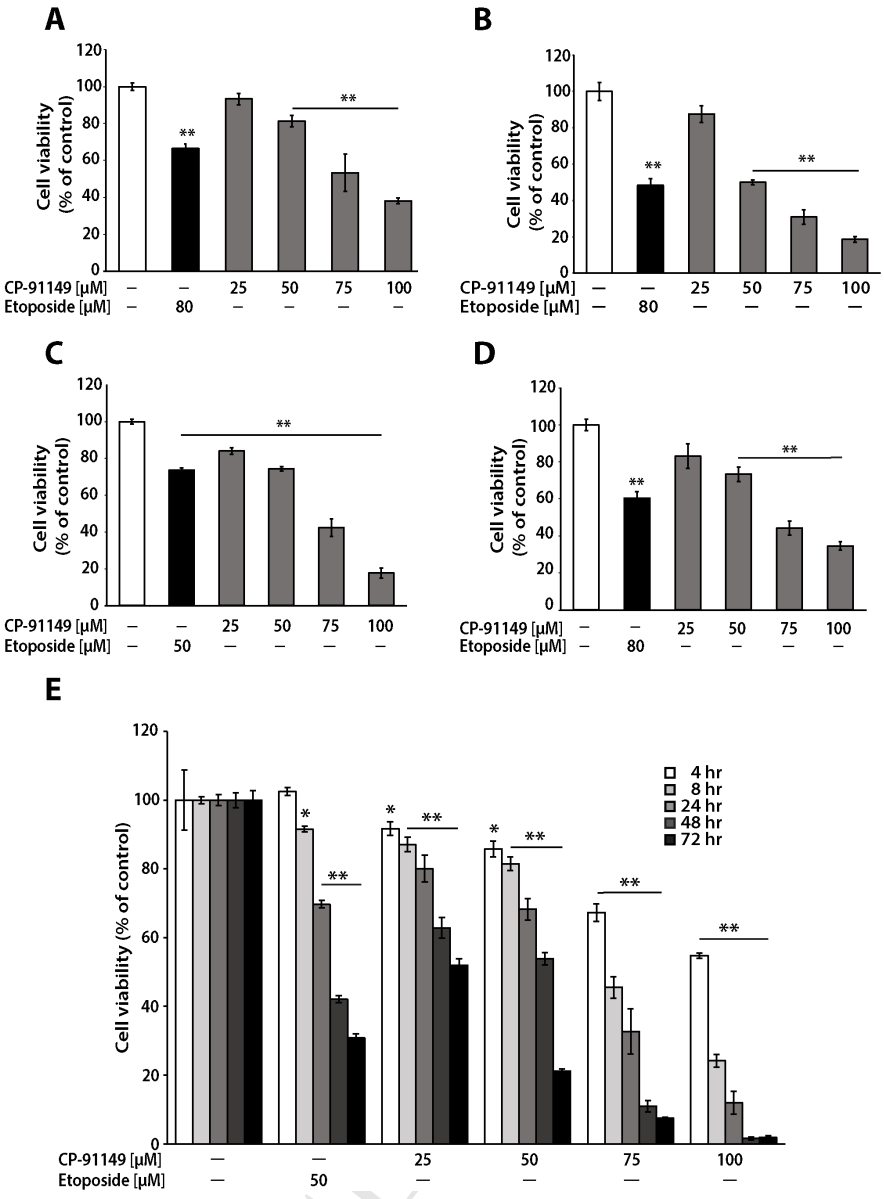
A
B
C
D
E
Cell viability (% of control)
CP-91149 [μM]
Etoposide [μM]
4 hr
8 hr
24 hr
48 hr
72 hr

Fig. 4

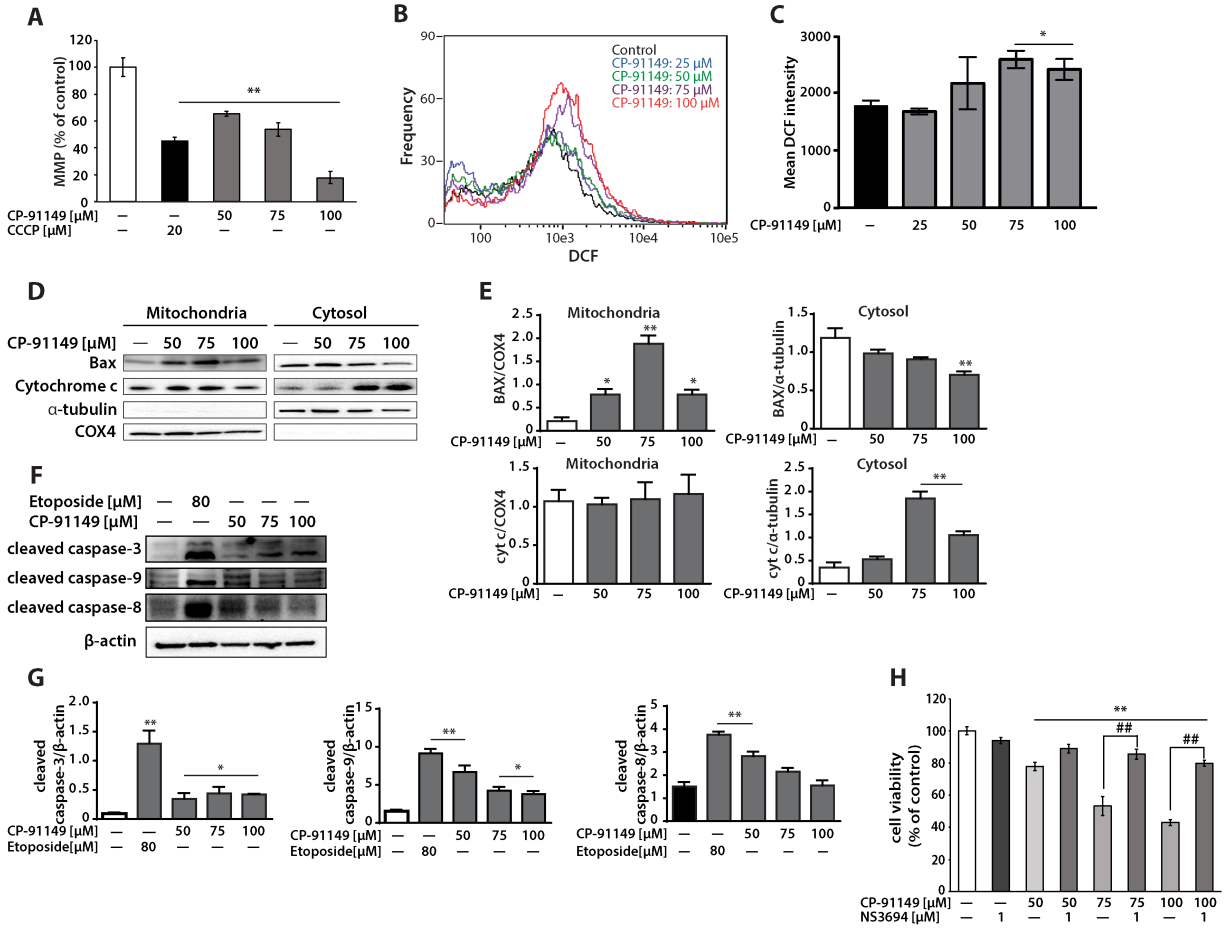

Fig. 5

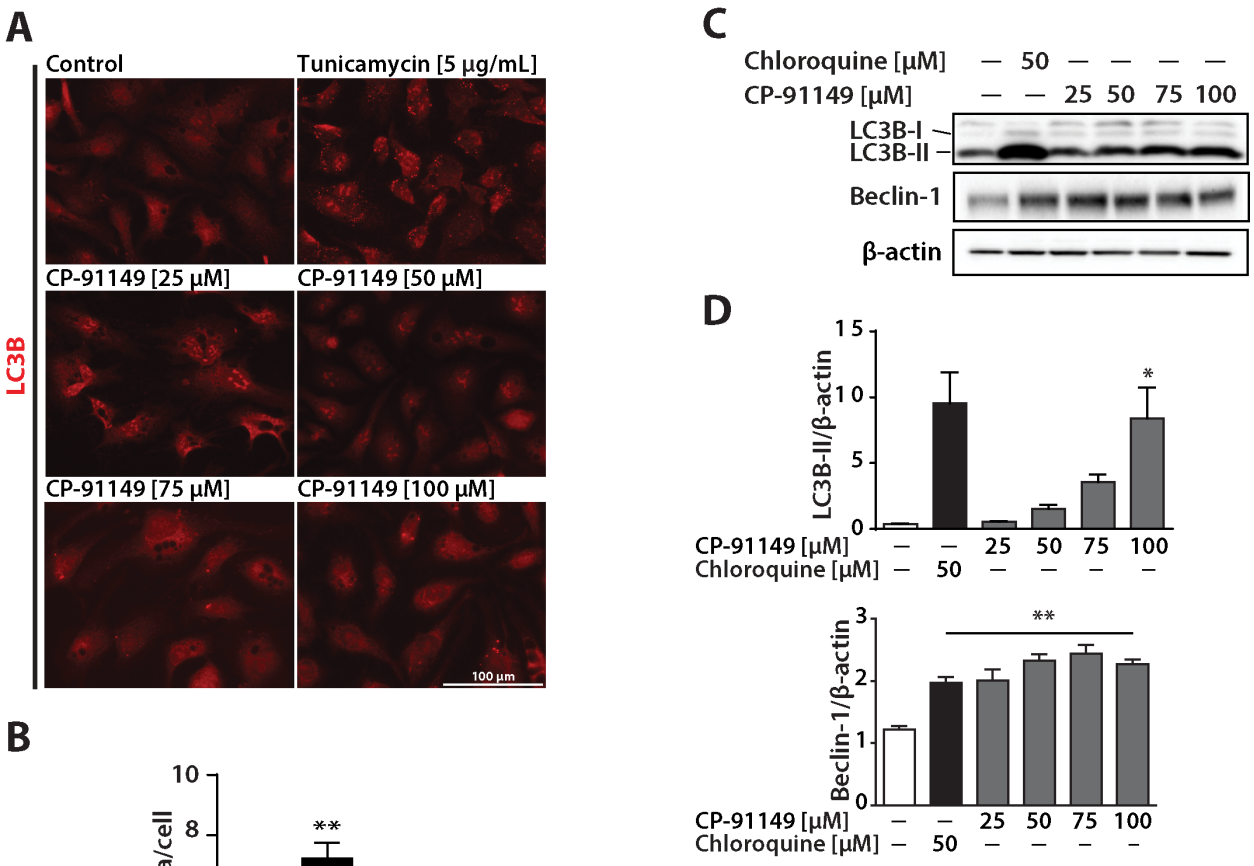
A
Control
Tunicamycin [5 μg/mL]
CP-91149 [25 μM]
CP-91149 [50 μM]
CP-91149 [75 μM]
CP-91149 [100 μM]
LC3B
100 μm
B
Average puncta/cell
10
8
6
4
2
0
**
**
CP-91149 [μM] – – 25 50 75 100
Tunicamycin [μg/ml] – 5 – – – –
C
Chloroquine [μM] – 50 – – – –
CP-91149 [μM] – – 25 50 75 100
LC3B-I
LC3B-II
Beclin-1
β-actin
D
LC3B-II/β-actin
15
10
5
0
*
CP-91149 [μM] – – 25 50 75 100
Chloroquine [μM] – 50 – – – –
Beclin-1/β-actin
3
2
1
0
**
CP-91149 [μM] – – 25 50 75 100
Chloroquine [μM] – 50 – – – –

Fig. 7

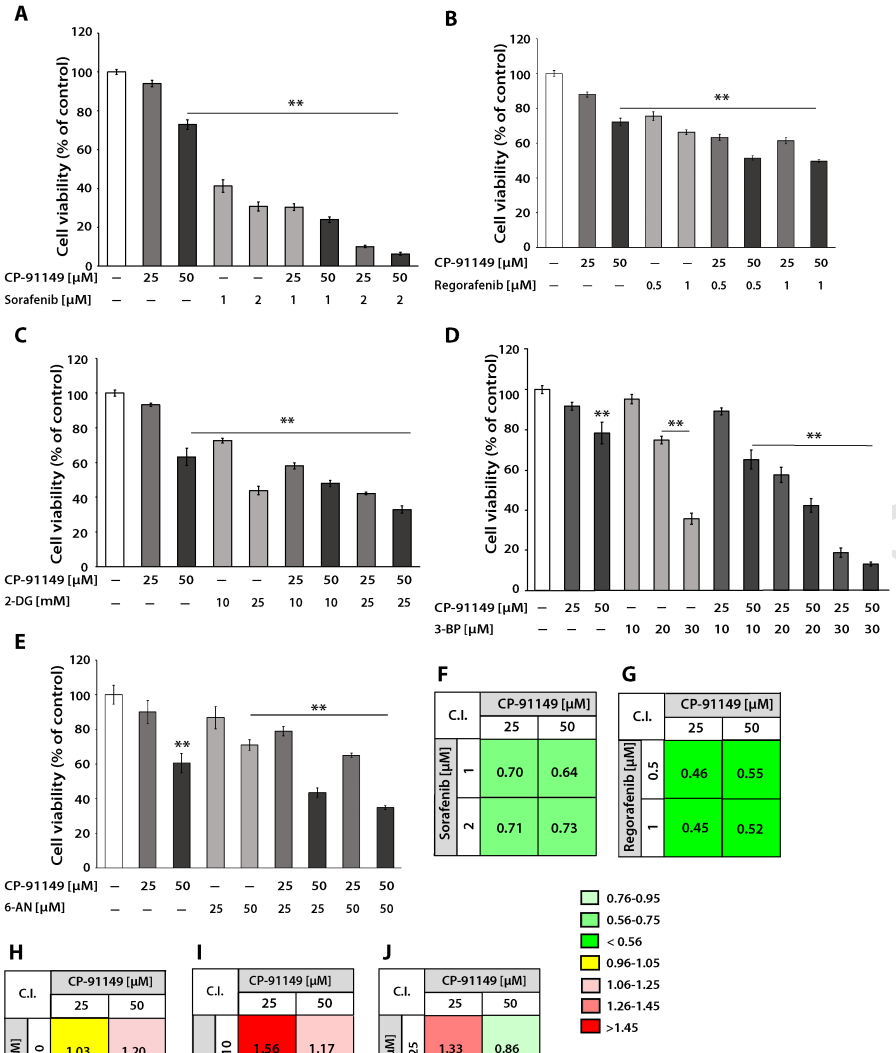

Fig. 2

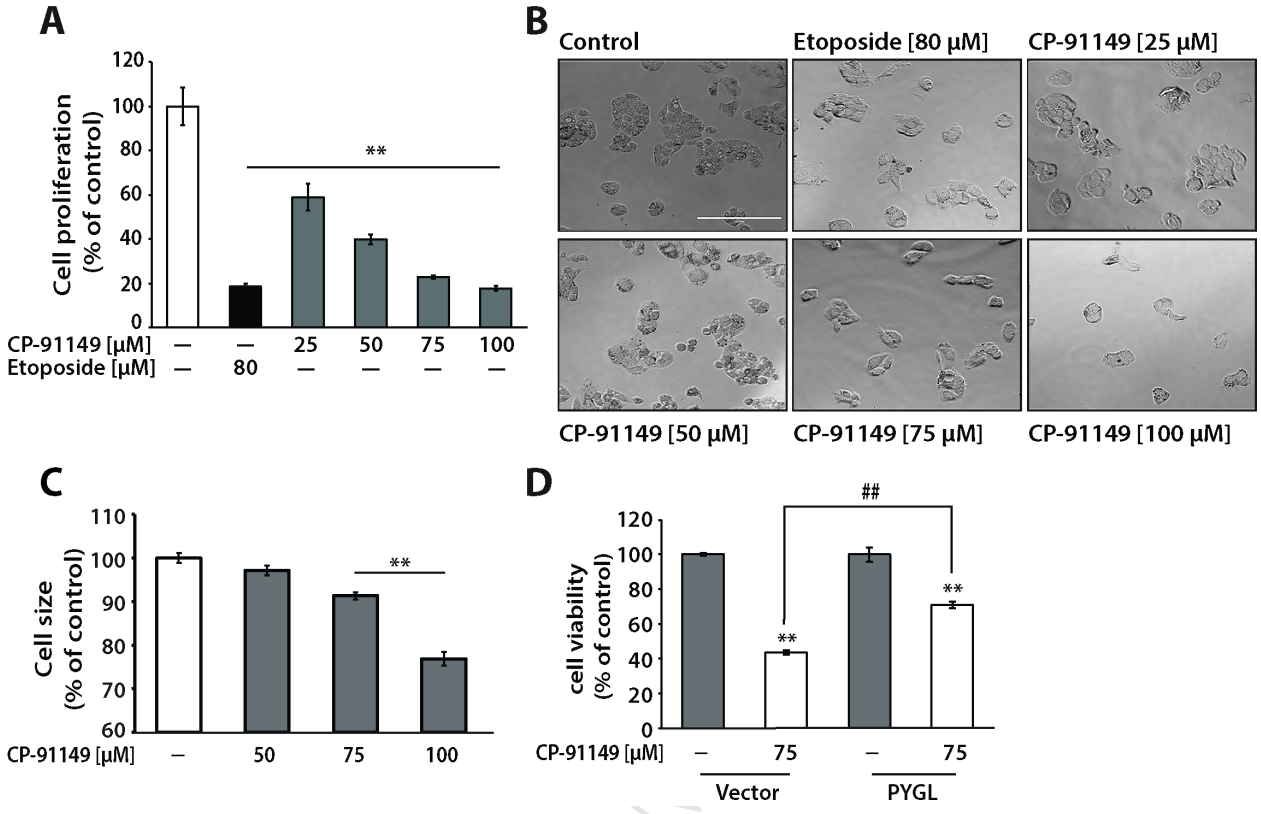

Fig. 6

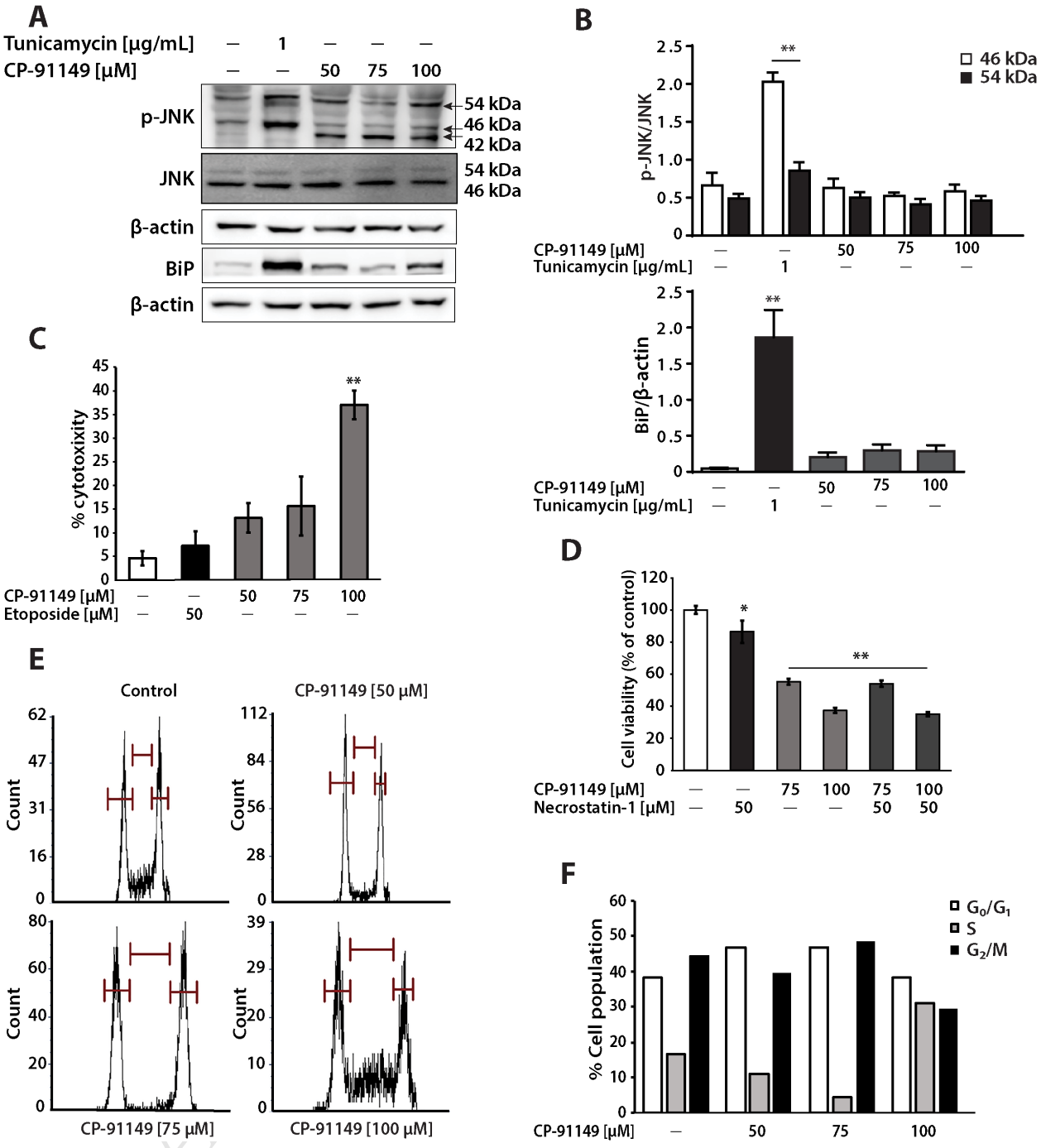
A
Tunicamycin [μg/mL] — 1 — — —
CP-91149 [μM] — — 50 75 100
p-JNK
JNK
β-actin
BiP
β-actin
54 kDa
46 kDa
42 kDa
54 kDa
46 kDa
B
p-JNK/JNK
46 kDa
54 kDa
**
CP-91149 [μM] — — 50 75 100
Tunicamycin [μg/mL] — 1 — — —
BiP/β-actin
**
CP-91149 [μM] — — 50 75 100
Tunicamycin [μg/mL] — 1 — — —
C
% cytotoxixity
**
CP-91149 [μM] — — 50 75 100
Etoposide [μM] — 50 — — —
D
Cell viability (% of control)
*
**
CP-91149 [μM] — — 75 100 75 100
Necrostatin-1 [μM] — 50 — — 50 50
E
Control
CP-91149 [50 μM]
Count
CP-91149 [75 μM]
CP-91149 [100 μM]
F
% Cell population
G0/G1
S
G2/M
CP-91149 [μM] — 50 75 100

Fig. 8

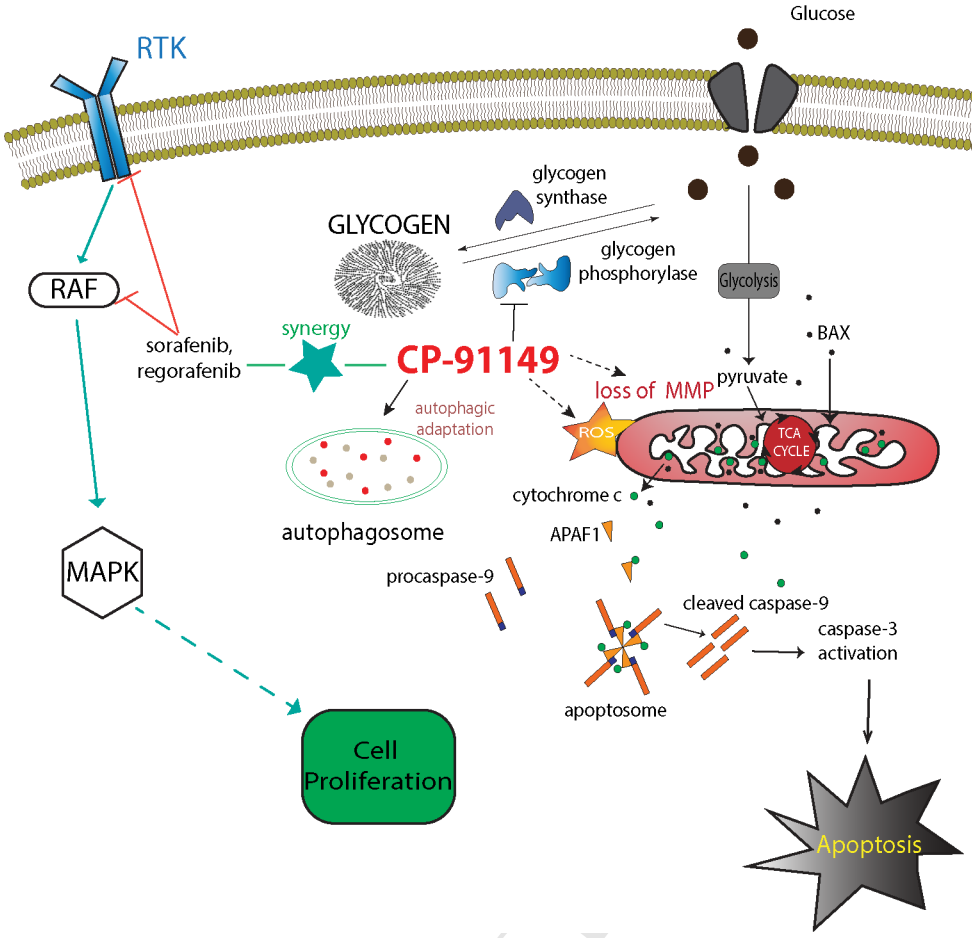

HIGHLIGHTS

Inhibition of glycogen catabolism induces intrinsic apoptosis and augments multikinase inhibitors in hepatocellular carcinoma cells

Shrikant Barot[a], Ehab M. Abo-Ali[a], Daisy Zhou[b], Christian Palaguachi[b], and Vikas V. Dukhande[a, *]

- Glycogen phosphorylase (GP) inhibition induces intrinsic apoptosis in liver cancer cells
- Mitochondrial dysfunctions- ROS generation and loss of MMP accompany apoptosis
- Autophagic adaptations are observed upon GP inhibition
- GP inhibition potentiates multikinase inhibitors in liver cancer cells